SOLAR PV ENERGY GENERATION SYSTEM INTERFACED TO THREE PHASE GRID WITH CPG

N. Sundara Perumal
PG Scholar, Department of Electrical and Electronics Engineering
Pandian Saraswathi Yadav Engineering College, Sivagangai, Tamil Nadu

S. Senthil Kumar
Assistant Professor Department of Electrical and Electronics Engineering
Pandian Saraswathi Yadav Engineering College, Sivagangai, Tamil Nadu

Abstract

This work deals with a multipurpose DS (Distributed Sparse) control approach for a single stage solar photovoltaic (PV) energy generation system (SPEGS). This SPEGS is interfaced here to the three phase grid at varying solar irradiance and compensating the nonlinear load tied at point of common interconnection. The SPEGS performs multitasks. It feeds the generated solar PV power to the local three phase grid. It reduces the harmonics of loads and furnished balanced currents of local three-phase grid. The SPEGS uses a solar PV array, a voltage source converter, a nonlinear load, a three phase grid, DC-link capacitance. In case, when the solar irradiance is not available, the proposed system works as DSTATCOM (Distribution Static Compensator) by utilizing same VSC (Voltage Source Converter). For extracting maximum power from the PV source, the traditional P&O (Perturb and Observe) scheme is utilized here. The tracking performance and efficiency of P&O technique are also examined here at rapid changing climatic conditions to show behavior of P&O scheme. The DS control approach is capable to estimate required fundamental component to find out reference grid currents. The proposed control approach is validated on a developed prototype in the laboratory.

Keywords: *Distributed Sparse Approach, Solar PV Power Generation, MPPT, VSC and Power Quality.*

Introduction

In general, due to increasing energy requirements, public awareness of climatic protection, the depletion nature of conventional resources, and the world political and social issues of nuclear power safety and because of lot of merits, solar PV (Photovoltaic) generation systems are getting increased attention [1]. Moreover, from last few decades, solar photovoltaic energy generation system (SPEGS) is one of the focused area of research community as it is pollution free, renewable, inexhaustible and has a lot of other advantages, which are discussed in [1-2]. The cost factor is one of the main aspect of any technology for its success or failure. Now a day, because of technology development, solar PV power is one of the feasible and alternative options among all non-traditional sources for power generation. The grid participation of solar PV power generation systems (SPEGSs), is reported in [3-4]. SPEGSs may be majorly divided in two categories, in which one is off-grid and another one is interfaced to the distribution feeder. However, due to the certain pitfalls of standalone SPEGSs, grid interfaced solar PV systems are more preferred [5, 6]. The non-linear relation between solar PV array voltage and its current, which depend on climatic condition, there is a need of MPPT (Maximum Power Point Tracking) scheme for harnessing the crest energy from the solar source. The initial expenditure of solar PV installation is also very high.

Hence, this is also one of the reason for harnessing the maximum power from total installed capacity. Various MPPT schemes are reported in the literature [7, 8]. However, due to simplicity and easy implementation, P & O (Perturb and Observe) scheme is more preferred [9]. In this work, the P&O method is utilized for extracting peak energy from the PV source.

Grid integrated SPEGSs are the systems, which harnesses the maximum power from the PV array and feeds that energy into the three phase grid. Moreover, there are various control methodologies, which are proposed by many research communities in the literature with various topologies [10-11]. These control techniques do not only serve for harnessing the maximum power from SPEGSs, however, they also work for grid synchronization and feed that harnessed power into three phase grid [11]. Hence, an improvement of control algorithm is the popular research area in this field [9-11].

In a current scenario, the power electronics based loads are increasing every day because of their certain advantages like efficiency and compactness [11-14]. The major demerits of these loads, are that they draw harmonics and reactive power from the distribution network, which deteriorate the power quality of the grid and increase the distribution losses [12-13]. To tackle such issues, many industries have utilized distribution static compensator (DSTATCOM), which serves for many purposes such as compensation of reactive power, harmonics minimization, load balancing, power factor correction etc. [14]. In practical application, its efficiency and performance mainly depend on its control algorithm [14]. However, the major pitfalls of such kind of devices, are their high cost. In this work, all these functions are performed by grid interfaced voltage source converter (VSC) in a very cost effective manner. Various control approaches such adaptive controls, neural network based algorithms are also proposed in the literature [15-18].

The distributed sparse (DS) control approach is widely applied in various fields to get the solution with learning and tracking capability. In [19], the authors have reported that conventional LMS (Least Mean Fourth) approaches do not exploit the sparsity in efficient way, which is solved by LMF (Least Mean Fourth) filter to some extent. However, its major pitfalls are that, its behaviour is influenced by noise and input. To solve this issue, a distributed based adaptive filter is proposed in [20-21]. In this approach, first, local normalized filter is improved by zero norms and it is extended for distributed processing for improvement in the estimation constant.

To mitigate the demerits and limitations of conventional least mean fourth (LMF) technique and to improve the convergence speed as well as the steady state performance, an adaptive sparse approach is developed here [20-21]. The salient features of this technique, are as follows.

- By extending the conventional normalized adaptive filter with cooperation factor, the estimation behaviour is improved [21].
- By inserting zero norms in local adaptive filter, the convergence rate, is enhanced as well as steady state behaviour is improved.
- The proposed approach improves the transient response.
- The proposed approach is based on peer-to-peer information estimation framework that is robust to link and node failure.

The proposed work deals with the distributed adaptive The proposed work deals with the distributed adaptive control approach for dual mode SPEGS integrated to the local three phase grid. The proposed technique works for two modes. In first mode, when sunlight is available, it harnesses the maximum power from the solar PV source and feeds that power three phase grid as well as connected load. Additionally in this mode, the same system configuration is also utilized for power quality improvement of the distribution network. In second mode, when sunlight is not present, it solely behaves as a DSTATCOM for mitigating the power quality issues of three phase grid with same VSC, which is used in first mode. So, in this way, power electronics devices are utilized to their maximum capacity and consequently, the payback time of proposed system is also reduced. The proposed algorithm has shown its potential to multitask such as mitigation of harmonics, improvement of power factor, load balancing along with unity power factor mode (UPF). Modelling and simulation of this control are done in MATLAB platform. For validating the proposed approach, a laboratory prototype is established to examine the performance under various test conditions such as variation in nonlinear loads, inaccessible of solar PV energy production at varying ambience situations. Moreover, the proposed approach also adheres the IEEE-519 standard [22].

Design and Control of the Proposed System

A multi-mode single stage SPEGS is depicted in Fig. 1. It comprises of a single converter, which is a voltage source converter (VSC) for harnessing optimum power via MPPT as well as to feed the solar power from source to the three phase weak distribution network and to assist it via facilitating some additional features like harmonics minimization, grid currents balancing and power factor improvement as a DSTATCOM without any additional device. Interfacing inductors are used between VSC and the distribution network to minimize the switching losses and subsequently, smoothens the distribution network currents. A high pass ripple filter is utilized at PCI (Point of Common Interconnection) to absorb the switching ripple produced at VSC. Detailed design and rating selection of different components, which are used in the proposed system, are made based on the procedure given in [14, 23]. Fig. 2 shows the proposed control of SPEG system interfaced to the three phase distribution network. This control consists of MPPT scheme and VSC switching. The MPPT scheme is achieved by P&O based scheme as well as the VSC control methodology is executed via adaptive based approach.

MPPT Algorithm

There are various MPPT methods reported in [8]. The P&O scheme is used in this work for harnessing maximum power from SPEGS [9]. The MPPT initially needs to take two points of solar panel voltage and solar array current and generates reference DC link voltage Vdc*.

Distributed Sparse based VSC Control

Fig. 2 provides the block of distributed sparse control for proposed system. Following variables are sensed for implementation of proposed control approach, which are PV voltage and current

(VPV, IPV), grid currents (i_{ga}, i_{gb}), load current (i_{La}, i_{Lb}) and a point of inter connection voltages (v_{ga} , v_{gb}). The amplitude of PCI voltage is obtained as,

$$V_t = \sqrt{\frac{2}{3}(v_{ga}^2 + v_{gb}^2 + v_{gc}^2)} \quad (1)$$

Where, the voltages of all three phases, are calculated from the recorded line voltages as,

$$v_{ga} = \frac{2v_{gab} + v_{gbc}}{3}; v_{gb} = \frac{-v_{gab} + v_{gbc}}{3}; v_{gc} = \frac{-v_{gab} - 2v_{gbc}}{3} \quad (2)$$

With the help of phase voltages, the in-phase unit templets are calculated as,

$$u_{pam} = \frac{v_{ga}}{V_t}; u_{pbm} = \frac{v_{gb}}{V_t}; u_{pcm} = \frac{v_{gc}}{V_t} \quad (3)$$

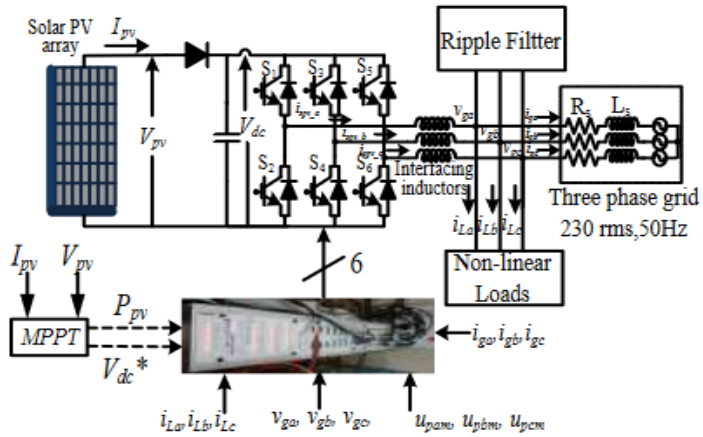

As it is given in [20, 21], utilizing distributed estimation method gives spatial diversity. Due to this, the performance in comparison with a local adaptive filter is improved. Therefore, for integrating a SPEGS into the grid, a novel distributive sparse based control technique is proposed in this section. The effectiveness of any distributed scheme is significantly influenced by co-operation that are allowed among the nodes [21]. In this case, a network is considered with m node adaptive technique. Here, the objective of everyone is to calculate the unspecified sparse vector Dwpa0.

In this scheme, as depicted in Fig.3, every node m, co- operates with its neighbor -hood nodes, Pm which is explained as a combination of nodes connected to node m with inclusion of node m also. By this approach, node m connectes to its local estimate, DWpam(n) with its neighborhood estimations, { DWlm(n), l belongs to Pm}, which is estimated as [21],

$$\lambda_{pam}(n) = \sum_{l \in p_m} \sigma_{lm} D_{Wlm} \quad (4)$$

Here em(n) denotes the error, which is reduced in every step by proper updation of the fundamental component of weight for load current.

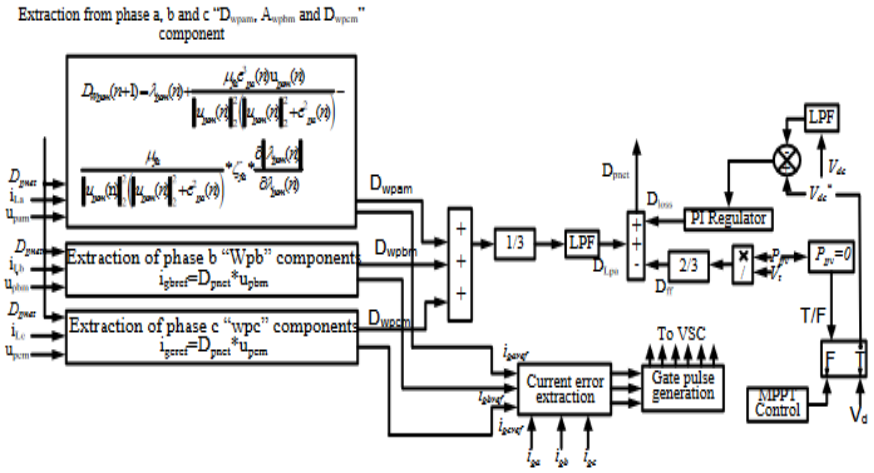

Figure 2 Block diagram for control architecture for SPEGS

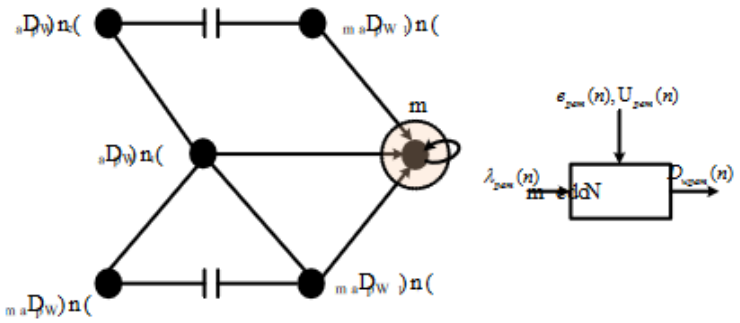

Figure 3 Block diagram of distributed sparse approach

In (4), the calculated estimation with cooperation factor, λ_{pam} at node m can feed into the local information and find final estimation Dwpam. Now, based on above error signal and calculated estimation with cooperation factor λpam at node m, the fundamental component of load current of phase 'a'is estimated as [19],

$$D_{wpam}(n+1) = \lambda_{pam}(n) + \frac{\mu_{fa} e^3_{pa}(n) u_{pam}(n)}{\|u_{pam}(n)\|_2^2 \left(\|u_{pam}(n)\|_2^2 + e^2_{pa}(n)\right)} - \frac{\mu_{fa}}{\|u_{pam}(n)\|_2^2 \left(\|u_{pam}(n)\|_2^2 + e^2_{pa}(n)\right)} * \zeta_{fa} * \frac{\partial \|\lambda_{pam}(n)\|}{\partial \lambda_{pam}(n)} \quad (6)$$

Similarly, for phase 'b' and phase 'c', the fundamental weight components of load currents are estimated as,

$$D_{wpbm}(n+1) = \lambda_{pbm}(n) + \frac{\mu_{fb} e^3_{pb}(n) \mathrm{u}_{pbm}(n)}{\|u_{pbm}(n)\|_2^2 \left(\|u_{pbm}(n)\|_2^2 + e^2_{pb}(n)\right)} - \frac{\mu_{fa}}{\|u_{pbm}(\mathrm{n})\|_2^2 \left(\|u_{pbm}(n)\|_2^2 + e^2_{pb}(n)\right)} * \zeta_{fb} * \frac{\partial \|\lambda_{pbm}(n)\|}{\partial \lambda_{pbm}(n)} \quad (7)$$

$$D_{wpcm}(n+1) = \lambda_{pcm}(n) + \frac{\mu_{fc} e^3_{pc}(n) u_{pcm}(n)}{\|U_{pcm}(n)\|_2^2 \left(\|U_{pcm}(n)\|_2^2 + e^2_{pc}(n)\right)} - \frac{\mu_{fc}}{\|u_{pcm}(n)\|_2^2 \left(\|u_{pcm}(n)\|_2^2 + e^2_{pc}(n)\right)} * \zeta_{fc} * \frac{\partial \|\lambda_{pcm}(n)\|}{\partial \lambda_{pcm}(n)} \quad (8)$$

Switching Pulses for VSC

By equating the sensed DC link voltage (Vdc) and estimated DC link voltage (Vdc*), the loss factor is obtained, which is given to the PI (Proportional-Integral) controller to control the DC link voltage to the defined value. The error is obtained as,

$$V_{dc\_error}(\mathrm{n}) = V_{dc}{}^*(\mathrm{n}) - V_{dc}(\mathrm{n})$$

Here, if solar power becomes unavailable (i.e. PPV=0), Vdc* moves to reference DC link voltage of DSTATCOM (Vdc* =Vdc_DS*) ,so that PV system functions as DSTATCOM when PV generation is not available in night time or in cloudy weather. In this case, same VSC works as a DSTATCOM, which is used for wheeling the active power from SPEGS to the distribution network as well as connected load without any additional equipment.

$$D_{ff} = \frac{2P_{pv}}{3V_t} \quad (11)$$

Here, V_t is amplitude of PCI voltage estimated in (1).

The active power component of utility grid (D_{Pnet}) is estimated as,

$$D_{pnet} = D_{Lpa} + D_{loss} - D_{ff} \quad (12)$$

Here, D_{Lpa} denotes the equivalent average load component of all three phase, which is calculated to perform load balancing and expressed as,

$$D_{Lpa} = \frac{\left(D_{wpam} + D_{wpbm} + D_{wpcm}\right)}{3} \quad (13)$$

Moreover, the reference currents for local distribution network are calculated as,

$$i_{garef} = D_{Lpa} * u_{pam} \; ; i_{gbref} = D_{Lpa} * u_{pbm} \; ; i_{gcref} = D_{Lpa} * u_{pcm} \quad (14)$$

An indirect current control approach with hysteresis controllers, is used to getting the switching pulses for VSC. Therefore, the current errors for hysteresis controller are calculated as,

$$i_{ga\_error} = i_{ga} - i_{garef} \; ; i_{gb\_error} = i_{gb} - i_{gbref} \; ; i_{gc\_error} = i_{gc} - i_{gcref} \quad (15)$$

Results and Discussion

For analyzing the behavior of PV energy generating system, a prototype is established in the laboratory. It includes of PV simulator, VSC, interfacing inductors, R-C filters, Hall-Effect sensors and nonlinear loads. The behavior of SPEGS is examined in various testing conditions, which are wheeling active power to the load in nominal condition, load perturbation condition, varying environmental conditions, during unavailability of solar insulation as a DSTATCOM with same VSC with its basic features for feeding the active energy from PV array to the utility. The DS algorithm is realized in real time on DSP-dSPACE controller. The value of different parameters, which are utilized in the hardware, are given in Appendices.

Response at Balanced Nonlinear Loading Condition

Fig. 4 depicts the behaviour of SPEGS under balanced nonlinear load. Fig. 4 (a) shows the three phase voltages (vgabc) with three phase grid currents (igabc). Three phase utility grid voltages and currents are in phase as well as maintained sinusoidal waveforms and almost equal in magnitude. Fig 4 (b) presents the details of three phase voltages, currents and grid power with power factor (PF). Fig. 4 (c) depicts vector diagram of balanced grid voltages (vgabc) and currents (igabc), which shows that the grid voltages and grid currents are placed from each other at equal angle. Fig. 4 (d) shows THD (Total Harmonics Distortion) of voltage (vgabc) and its current (igabc), which is found satisfactory and in range of the IEEE 519- std. Fig 4 (e) presents the waveforms of grid voltages (vgabc) and VSC currents (ivsc). Fig 4 (f) shows the three phase voltages and VSC currents with VSC power, PF and PQ (Power Quality) information. Fig. 4 (g) depicts the three phase voltages (vgabc) with load currents (igabc), which are quasi-square in shape and equal in magnitude. Fig. 4

(h) shows the three phase voltages and load power with PF and PQ information. The total harvested power from the PV array beside consumed by the load, is fed to the distribution feeder via VSC. Fig. 4 (i) presents the THD of grid voltage and load current of phases 'a'. After regressive examination of Fig. 4, it is found that the grid voltages and currents are balanced and perfect sinusoidal with PF near to unity. THD values of grid voltages and currents are found in acceptable range of the IEEE-519 standard [22] and the system operates satisfactory.

Experimental Results at Unbalanced Nonlinear Load

The behaviour of proposed system at unbalanced nonlinear load. Fig. 5 (a) shows the three phase voltages (vgabc) with three phases grid currents (igabc). Three phase voltages and currents are in phase as well as maintained sinusoidal waveforms and almost equal in magnitude. However, the load currents are unbalanced. Fig 5 (b) provides the detail of three phase voltages, currents and grid power with power factor (PF), which are satisfactory. Fig. 5 (c) depicts vector diagram of balanced grid voltages (vgabc) and currents (igabc). Fig. 5 (d) depicts THD (Total Harmonics Distortion) of voltages (vgabc) and its currents (igabc). Fig.5 (e) depicts the THD value of iga upto 50^{th} harmonics, which is found satisfacory and in range of the IEEE std.-519. Fig 5 (f) depicts the grid voltages (vgabc) and VSC currents (ivsc). Fig 5 (g) shows the three phase voltages and VSC currents with PF and PQ (Power Quality) information. Fig. 5 (h) depicts the vector diagram of three phase balanced voltages and VSC currents, which depicts that the grid voltages are placed from each other at equal angle. Fig. 5 (i) shows the three phase grid voltage (vgabc) with load currents (igabc). Fig. 5 (j) depicts the three phase voltages and load currents with PF and PQ information. Fig. 5 (k) depicts the vector diagram of three phase balanced voltages and load currents, which are quasi-square in shape. The total harvested energy is fed to the utiltiy and load via multifunctional VSC. Figs. 5 (l) gives THD value of voltages and load currents of phases 'a'. After regressive examination of Fig. 5, it is noticed that the grid voltages and currents are identical in magnitude as well as balanced and perfect sinusoidal with PF near to unity. THDs of voltages and currents are found in acceptable range of the IEEE-519 standard [22] and the system operates satisfactory.

DS Control Approach Behaviour

Different intermediate signals are shown Figures to analyze the behaviour of proposed DS approach. Figures presents the load current (iLa), product of unit template for phase 'a, and extracted load current components (upam*DWpam), error (epam), product of unit template for phase 'a and error cube (upam*epa Fig. 6(b) shows the load current (iLa), effect of constant (ζpa), fundamental load current component with co-operation factor (λpam) and unit template (upam). Fig. 6(c) depicts the load current (iLa), weight for distributed average component of load (DLpa), weight of active loss factor (Dloss) and weight of net active component (Dpnet). Here, it is found that on addition of load, average component is increased and all other intermediate signals are settled to their steady-state value. Additionally, Figures reveal the performance of system during sudden removal of loads. In this case, it is also found that every intermediate signal and load current are settled to steady-state

value on removal of load of phase 'a', which means dynamic performance of SPEGS is quick and satisfactory. It means that the load current (iLa) is instantly settled to zero and all the other signals achieve their steady-state value after disconnection of load from phase 'a'.

Dynamic behaviour of Solar PV Energy Generation System

Figure depicts the response of SPEGS at nonlinear load perturbation. Here, Figures show the system behavior at sudden addition of loads. Figures depicts the waveforms of load current (iLa), weight of feed-forward term (Dff), reference grid current (igrefa), sensed grid current (iga), respectively. Figures depicts signals of load currents (iLa, iLb, iLc) for phase 'a-c', respectively. Whereas, Figures shows the load current for phase 'a' (iLa), grid current (iga), VSC current (ivsca) and PV current (ipv), respectively. Here, it is found that the reference grid current is decreased on load addition and followed by sensed grid current. Moreover, other signals are settled at their steady-state value. Figures show the system performance during sudden removal of loads. In this case, it is found that, reference grid currents are increased and followed by sensed grid currents, because the extra power is fed to the grid.

Dynamic Performance at Varying Climatic Condition

Figures depicts the system behaviour at varying climatic condition from 1000 W/m^2 to 500 W/m^2. Here, it is found that on the solar irradiance decrease, subsequently, the PV power falls and the DC link voltage is sustained to its desired value. Furthermore, the amplitude of grid currents falls, but it is still maintained its sinusoidal shape. Fig. 8 (b) shows the system performance during sudden increase of PV insolation from 500 W/m^2 to 1000 W/m^2. Here, it is noticed that the energy fed to the distribution network, is increased on an increment in insolation level. The DC link voltage is maintained at its desired value and the grid currents are sustained to be sinusoidal. Here, the feed-forward term is calculated the control output accurately in a presumed manner. Moreover, Figs. 9(a-b) present the MPPT percentage at 1000 W/m^2 and 500 W/m^2, which is 100 %.

System Performance as DSTATCOM

One important feature of this system, is that it should not only produce power only for some duration of the time when solar Generation is present, but rest of the time, when solar rays are not available it acts as a DSTATCOM with same VSC,

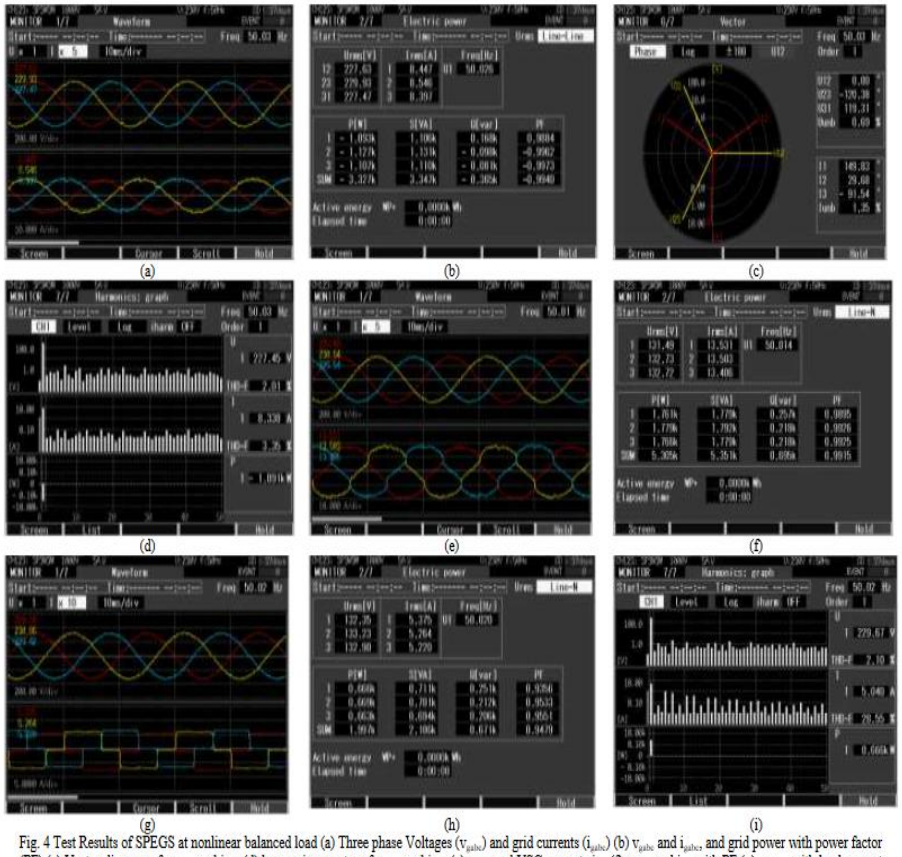

Fig. 4 Test Results of SPEGS at nonlinear balanced load (a) Three phase Voltages (v_{gabc}) and grid currents (i_{gabc}) (b) v_{gabc} and i_{gabc}, and grid power with power factor (PF) (c) Vector diagram of v_{gabc} and i_{gabc} (d) harmonics spectra of v_{gabc} and i_{gabc} (e) v_{gabc} and VSC currents i_{vsc} (f) v_{gabc} and i_{vsc} with PF (g) v_{gabc} with load current (i_{Labc}) (h) v_{gabc} & i_{Labc} with load power and PQ detail (i) THD of v_{gabc} and i_{Labc} .

Which is utilized to feed the active power from solar PV source to the distribution network. Figures present the dynamic response of SPEGS, when the solar power is not available and when the PV power is recovered on solar light availability. It is noticed in Figures, when the PV power is not available (Vdc= Vmp to Vocn) and VSC gives compensating currents (ivsc). It acts as a DSTATCOM for grid self-healing. Whereas, distribution grid currents are decreased and their phase is reversed and DC link voltage is sustained at its recommended value. These grid currents are sinusoidal and after few cycles, phase becomes reverse. Figures depicts the system performance after solar PV power is regained.

Comparative Study of Proposed DS Control Approach with Existing Control Methods

For doing this, the SPEGS is subjected to the load disconnection in phase ‘a’ at .4s. The fundamental weight component of proposed distributed sparse based control approach with traditional approaches namely [24]-[27] LMS and LMF are illustrated in Fig. 11. Fig. 11 clearly shows that proposed control approach performance is better than existing algorithms like ILST, PLL-Less, FZANLMF control methods. Here, it is also found that in proposed control method, fast convergence is achieved than other existing control methods such as ILST, LMS, PLL-Less,

FZANLMF in unbalancing loading conditions, nominal conditions as well as rapidly varying ambience situations. These test results clearly reveal that proposed DS (Distributed Sparse) based control approach has excellent efficiency in weight calculation because of co- operation factor. Moreover, the detailed performance evaluation of proposed DS based control scheme with existing methods such as ILST[24], LMS[25], PLL-Less [26], FZANLMF [27] and LMF[9] for SPEGS integration in local distribution feeder, is given in Table-I. It is also observed that for particular moment, the mean square error (MSE) is very small for proposed approach than existing controls in any critical examined condition as well as nominal operating condition. Here, the novelty of this algorithm, is that the neighbor of node m gives as the set of nodes directly linked to it, including the node m also. Every individual node m, takes advise from peer nodes from its neighborhood and combines their past estimate with its own past estimates, as in (4) as well as in error estimation (5) [20, 21].

After that, node produces an aggregate estimate and sends it in local adaptive filter, as in (6). Due to which, estimation becomes more robust and intelligent [20, 21]. However, in [9, 24 and 25], it is found that the proposed control shows its potential during weak distribution system conditions. Whereas, the proposed control algorithm shows its potential during weak grid conditions. The performance of control technique is verified experimentally under voltage sag and swell conditions as shown in Figs. 12(a)-(b). In Fig. 12 (a), a 20 % sag is applied on grid voltage, due to this, the grid current is increased on same amount and system operates satisfactory. Whereas, Fig. 12 (b) shows a 20 % swell condition in grid voltage, due to which grid current is decreased by same amount and the system works well. Furthermore, this system with proposed control approach also works as a DSTATCOM, in the absence of solar power, which is not shown in existing control algorithms such as ILST [24], LMS [25] and LMF [9]. The grid current is increased and decreased under voltage sag and swell condition to maintain a constant power fed to the grid and remains sinusoidal. No significant effect is observed in the PV voltage, current and output power under change in voltage.

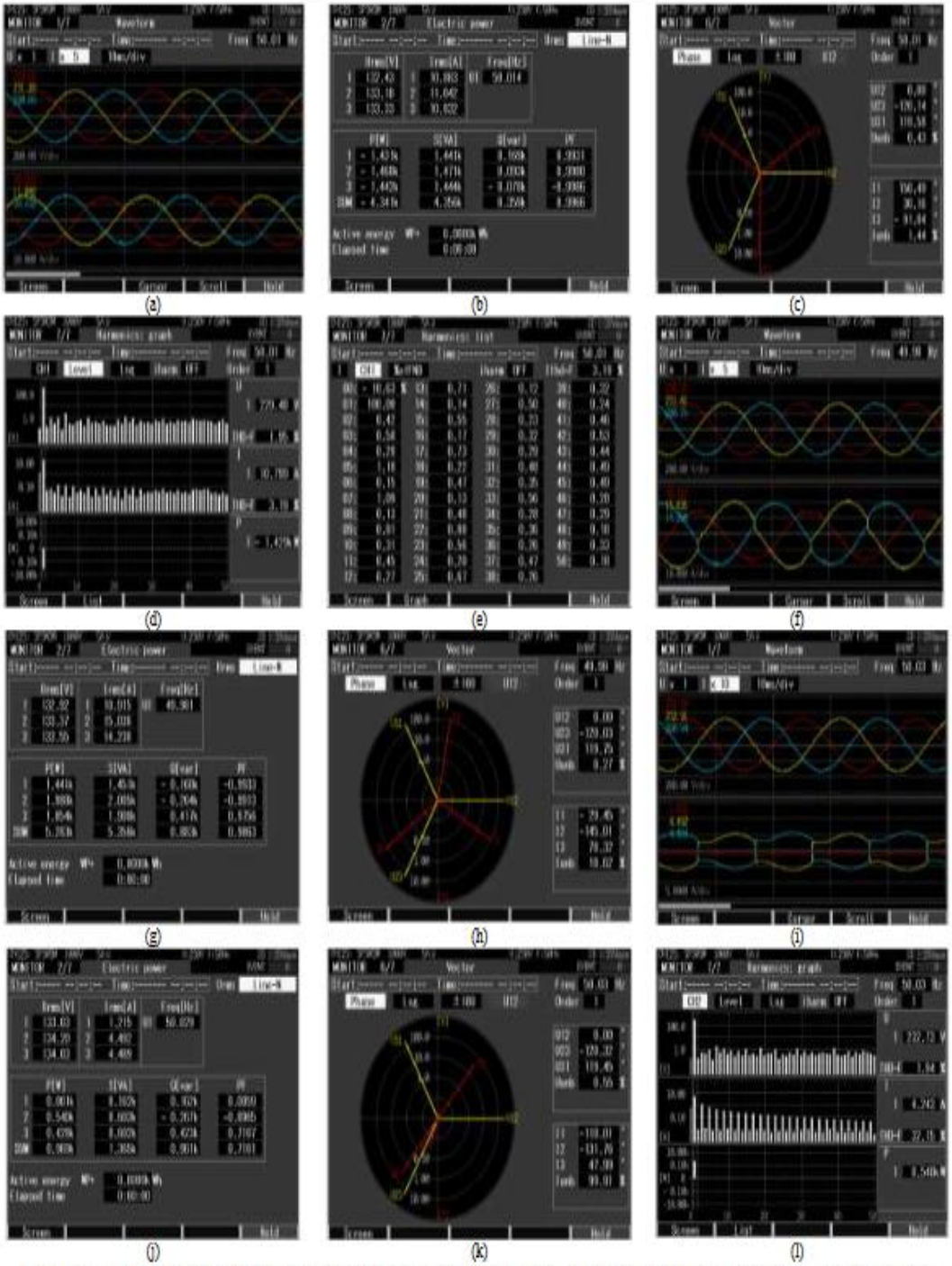

Fig. 5 Test validation of SPEGS during nonlinear unbalanced load (a) Three phase Voltages (v_{gabc}) and grid currents (i_{gabc}) (b) vgabc and i_{gbcn} and load power with power factor (PF) (c) Vector Diagram of v_{gabc} and i_{cabc} (d) THD of v_{gabc} and i_{gabc} (e) THD value of i_{gc} upto 50th harmonics (f) v_{gabc} and VSC currents i_{cc} (g) VSC power with PF (h) Vector diagram of v_{gabc} and i_{cac_abc} (i) unbalanced load currents with grid voltages (j) load power under unbalanced conditons (k) Vector Diagram of v_{gabc} and i_{cabc} under unbalanced conditons (l) harmonics spectra of load current and grid voltage

TABLE-I
COMPARATIVE ANALYSIS OF PROPOSED DISTRIBUTED SPARSE APPROACH WITH EXISTING CONTROL APPROACHES (Technical and Economical Comparison)

Parameters	Conventional And Existing Adaptive Control Approach					Proposed Approach (Distributed Sparse based Approach)
	ILST [24]	PLL-Less [26]	FZA-NLMF [27]	LMS [25]	LMF [9]	
Type of Filter	PLL-Less	PLL-Less	PLL-Less	Adaptive Technique Based Filter, PLL Less	Adaptive Technique Based Filter, PLL Less	Adaptive Technique Based Filter, PLL Less
Complexity	More	More	Less	Small	Small	Small
Optimization Order	NA	NA	4_{th} order	2_{nd} order	4_{th} order	4_{th} order
Static error	Better	Better	Less	High	High	Small
Oscillation	High	Midum		High	Less	Very Less
dSpace Speed	Low	Low	High	High	High	High
MSE	NA	NA	8.07	19.79 [9]	17.02 [9]	5.05
Computational Load	High	High	Less	Less	Less	Less
Sampling time (Ts)	50µs	50µs	30µs	30µs	30µs	30µs
Settling time	.16s	.2s	.09s	.1s	.1s	.07s
THD in grid current	3.3 % [24]	4.6 %	1.13 %	1.26% [25]	1.12% [9]	1.01%
Performance During night Time, When PV Power is not available	Not Performed [24]	Not Performed	Not Performed	Not Performed [25]	Not Performed [9]	Performance Satisfactory, in the absence of PV power, shown in section III (F)
Performance During Weak Grid Condition	Not Performed [24]	Not Performed [3]	Not Performed [4]	Not Performed [25]	Not Performed [25]	Performance Satisfactory during Sag and Swell in grid voltage, shown in Fig. 12
Cost	High (Because of Two Stage Converter	High (Because of Two Stage Converter	High (Because of Two Stage Converter	Less (Because of Single Stage Converter	Less (Because of Single Stage Converter	Less (Because of Single Stage Converter
Power Converter Utilization	Less (Because, When Solar PV Energy not avilable, System shut down	Less (Because, When Solar PV Energy not avilable, System shut down	Less (Because, When Solar PV Energy not avilable, System shut down	Less (Because, When Solar PV Energy not avilable, System shut down	Less (Because, When Solar PV Energy not avilable, System shut down	100 % (Because, When Solar PV Energy not avilable, System behave as a DSTATCOM
Pay Back Time	High	High	High	High	High	Less compared to existing approaches

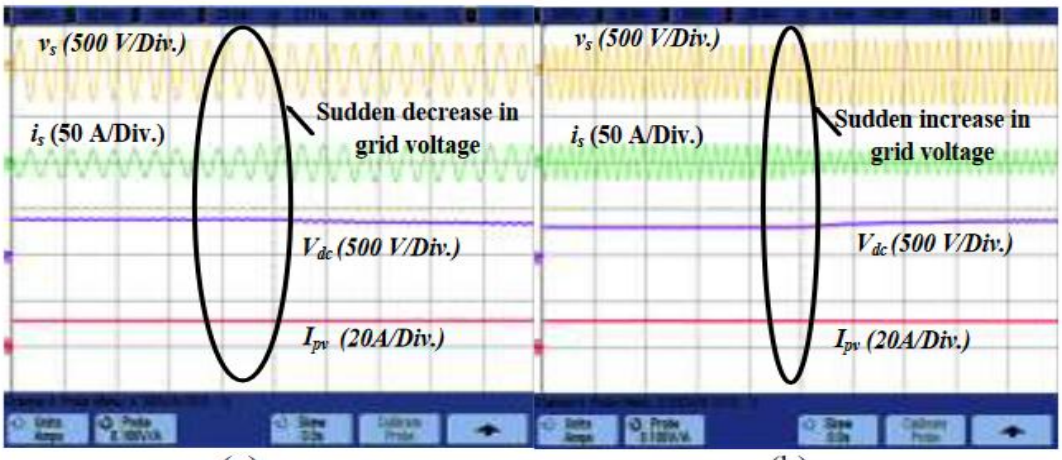

(a) (b)

Fig. 12 (a)-(b) Experimental Performance during sag and swell in grid voltage

Conclusion

A multimode single stage SPEGS interfaced to a distribution feeder using robust distributed sparse based control approach has been developed for improving power quality. Exhaustive experiments have been performed for the validation of the system. The main aspects of distributed sparse approach are its simplicity and robustness. The proposed system is tested at nonlinear load, unbalanced load, existence, and non-existence of solar rays and varying insolation level. In experimental results, it is observed that adaptive sparse control approach is better for extraction of active load current component of multimode SPEGS. Dynamic behaviour of proposed control technique, has been observed better in comparison with existing control approaches. The proposed approach has worked well in all scenarios at unity power factor operation and resolves proplems related to power quality of grid. The THD of grid currents, is obtained in the limit of the IEEE-519 standard [22

Appendix A

System Parameters for Simulation: Vdc = 700 V; DC link capacitance, Cdc = 6 mF; interfacing inductance, Lf = 2.5 mH; Grid voltage, VL-L = 415 V (rms); PI controller gains Kp=.64; Ki=.4.Experimental System Parameters: PV array voltage, VMP = 387.54 V; IMPP = 15.168 A; PMPP = 5.878 kW; Vdc = 380 V; Lf = 2.4 mH, Ts = 30 μs, VLL = 227.47 V (rms); Rf =5 Ω and Cf=10 μF, Kpd=0.04 and Kid= 0.01, PI controller, Kp = 0.68 and Ki = 0.4; adaptive step constant, μf = 0.0001 and K=.01, co-operation coefficient, □lm=.01, LPF cut-off frequency fc= 10 Hz.

Appendix B

Case Study: Comparative Study of Proposed DS Control with and Without PVFFT

Fig. 13 illustrates the behavior of SPEGS with and without PV feed-forward term (PVFFT) to perceive the usefulness of DS (Distributed Sparse) based algorithm at sudden variation in solar irradiance. The behavior DS based control algorithm with PVFFT, is demonstrated in Fig.13 (a). The sudden increase in irradiance from 500 W/m^2 to 1000 W/m^2 is noticed at 0.5 s. The change in DC link voltage (Vdc), is not perceived and hence, burden on PI regulator is minimized. Furthermore, the variation in the utility currents (is) are not perceived at step variation at solar irradiance. Nevertheless, the utility currents are increased as energy fed to the utility is increased.

The oscillations in utility voltages (*vs*) are also not perceived at varying irradiance. Fig. 13 (b) demonstrates the response of conventional algorithm without PVFFT. There is an observable (around 60 V) overshoot and undershoot in (Vdc), which puts the burden on PI regulator. Nevertheless, the PVFFT prediction observes the net results accurately in pre-defined way. The task of PI regulator is to reduce the voltage variation between the existing conditions of SPEGS and the actual state, which requires to reduce the voltage difference. The difference between sensed *Vdc* and *Vdc* * increases the energy loss in DC link of VSC. The variations in the utility currents are also perceived at variation in solar irradiance, which increases the losses and tripping of VSC.

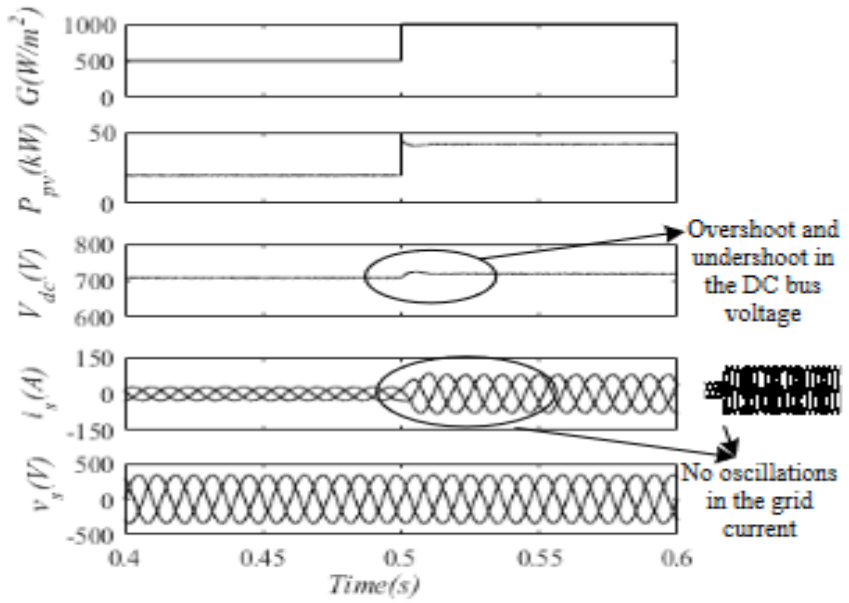

Fig.13 Comparative analysis of distributed sparse and conventional algorithm (a) with PVFFT and (b) without PVFFT

References

1. L Robert Foster, Majid Ghassemi and Alma Cota, "Solar Energy Renewable Energy and the Environment," CRC Press FL 2010.
2. F.A. Farret and M.G. Simões, Integration of Alternative Sources of Energy, John Wiley & Sons, Inc., 2006.
3. Mu Zhou, "Report for reviewing the renewable energy and energy saving in USA", *Journal of*

Renewable Energy, vol. 25, no.1, PP. 98-101, 2007.

4. S. Reichelstein and M. Yorston, "The prospects for cost competitive solar PV power special section: Long run transitions to sustainable economic structures in the European Union and beyond," *Energy Policy,* vol. 55, pp. 117–127, 2013.
5. F. Locment, M. Sechilariu and I. Houssamo, "DC Load and Batteries Control Limitations for Photovoltaic Systems. Experimental Validation," *IEEE Trans. Power Electronics,* vol. 27, no. 9, pp.4030, 4038, Sept. 2012.
6. Caisheng Wang and M. H. Nehrir, "Power Management of a Stand-Alone Wind/Photovoltaic/Fuel Cell Energy System," *IEEE Transactions on Energy Conversion,* vol. 23, no. 3, pp. 957-967, Sept. 2008.
7. S. Jain and V. Agarwal, "Comparison of the performance of maximum power point tracking schemes applied to single-stage grid-connected photovoltaic systems," *IET Electric Power Applications*, vol. 1, no. 5, pp. 753-762, Sept. 2007.
8. Subudhi and R. Pradhan, "A Comparative Study on Maximum Power Point Tracking Techniques for Photovoltaic Power Systems," *IEEE Transactions on Sustainable Energy*, vol. 4, no. 1, pp. 89-98, Jan. 2013.
9. R. K. Agarwal, I. Hussain and B. Singh, "LMF-Based Control Algorithm for Single Stage Three-Phase Grid Integrated Solar PV System*," IEEE Trans. Sustainable Energy*, vol. 7, no. 4, pp. 1379-1387, Oct. 2016.
10. S.B. Kjaer, J.K. Pedersen, F. Blaabjerg, "A review of single-phase grid- connected inverters for photovoltaic modules," *IEEE Transactions on Industry Applications,* vol.41, no.5, pp.1292-1306, Sept.-Oct. 2005.
11. F. Chan and H. Calleja, "Reliability Estimation of Three Single-Phase Topologies in Grid Connected PV Systems," *IEEE Transactions on Industrial Electronics,* vol.58, no.7, pp.2683-2689, July 2011.
12. Antonio Moreno Munoz, Power Quality: Mitigation Technologies in a Distributed Environment, Springer-Verlag, London, 2007.
13. Ambra Sannino, Jan Svensson and Tomas Larsson,"Review power- electronic solutions to power quality problems,"*Journal of Electric Power Systems Research,* vol. 66, pp.71-82, 2003.
14. Singh, A. Chandra, and K. Al-Haddad, Power Quality: Problems and Mitigation Techniques. Chichester, U.K.: Wiley, 2015.
15. B. Singh, S. K. Dube, S. R. Arya, A. Chandra and K. Al-Haddad, "A comparative study of adaptive control algorithms in Distribution Static Compensator," *in Proc. of IEEE Annual Conference of Industrial Electronics Society (IECON)*, 2013, pp.145-150.
16. Parmod Kumar and A. Mahajan, "Soft Computing Techniques for the Control of an Active Power Filter," *IEEE Transactions on Power Delivery,* vol.24, no.1, pp.452-461, Jan. 2009.
17. Chao-Shun Chen, Chia-Hung Lin, Wei-Lin Hsieh, Cheng-Ting Hsu and Te-Tien Ku, "Enhancement of PV Penetration With DSTATCOM in Taipower Distribution System," *IEEE Transactions on Power Systems,* vol.28, no.2, pp.1560-1567, May 2013.

18. B. Singh, D. T. Shahani and A. K. Verma, "Neural Network Controlled Grid Interfaced Solar Photovoltaic Power Generation," *IET Power Electronics*, vol.7, no.3, pp. 614-626, July 2013.
19. G. Lopes and A. H. Sayed, "Diffusion Least-Mean Squares Over Adaptive Networks," *IEEE Intern. Conf. Acoustics, Speech and Signal Processing* - ICASSP '07, Honolulu, HI, 2007, pp. III 917-III-920.
20. H. Sayed and C. G. Lopes, "Distributed processing over adaptive networks," *9th International Symposium on Signal Processing and Its Applications*, Sharjah, 2007, pp. 1-3.
21. M. Hajiabadi and H. Zamiri-Jafarian, "Distributed adaptive LMF algorithm for sparse parameter estimation in Gaussian mixture noise," *7'th Inter. Symp. Telecommun. (IST'2014)*, Tehran, 2014, pp. 1046-1049.
22. IEEE Recommended Practices and requirement for Harmonic Control on Electric Power System, IEEE Std.519, 1992.
23. M. Villalva, J. Gazoli and E. Filho, "Comprehensive approach to modeling and simulation of photovoltaic arrays," *IEEE Trans. Pow. Elec*., vol.24, no.5, pp.1198-1208, May 2009.
24. B. Singh, C. Jain and S. Goel, "ILST Control Algorithm of Single-Stage Dual Purpose Grid Connected Solar PV System," *IEEE Transactions on Power Electronics*, vol. 29, no. 10, pp. 5347 5357, Oct. 2014.
25. R. K. Agarwal, I. Hussain and B. Singh, "Integration of single-stage SPV generation to grid using admittance based LMS technique," *International Conference on Emerging Trends in Electrical Electronics & Sustainable Energy Systems (ICETEESES), Sultanpur*, 2016, pp. 308-313, 2016..
26. S. Deo, C. Jain and B. Singh, "A PLL-Less Scheme for Single-Phase Grid Interfaced Load Compensating Solar PV Generation System," *IEEE Trans. Industrial Informatics*, vol. 11, no. 3, pp. 692-699, June 2015.
27. Amresh Kumar Singh, I. Hussain and B. Singh, "Double-Stage Three- Phase Grid-Integrated Solar PV System With Fast Zero Attracting Normalized Least Mean Fourth Based Adaptive Control," *IEEE Trans. Industrial Electronics*, vol. 65, no. 5, pp. 3921-3931, May 2018.